Emergence of Bloch Bands in a Rotating Bose-Einstein Condensate

Hiroki Saito and Masahito Ueda

Department of Physics, Tokyo Institute of Technology, Tokyo 152-8551, Japan
and CREST, Japan Science and Technology Corporation (JST), Saitama 332-0012, Japan

(Received 13 January 2004; published 23 November 2004)

A rotating Bose-Einstein condensate is shown to exhibit a Bloch band structure even in the absence of a periodic potential. Vortices enter the condensate via Bragg reflection if the frequency of a rotating drive is adiabatically increased or *decreased*, or if the interaction is adiabatically changed at a constant rotating drive. A localized state analogous to a gap soliton in a periodic system is predicted to occur near the edge of the Brillouin zone.

DOI: 10.1103/PhysRevLett.93.220402 PACS numbers: 03.75.Lm, 03.75.Kk, 32.80.Pj, 67.40.Vs

The Bloch band is crucial to our understanding of periodic systems, such as electronic states in solids [1], atom dynamics in optical lattices [2], and Cooper-pair tunneling in small Josephson junctions [3]. The underlying physics common to all of these is the Bragg reflection that occurs at the edges of the Brillouin zone. The resultant Bloch band gives rise to various interesting phenomena, such as Bloch oscillations [1] (wherein a particle in a periodic potential driven by a weak constant force cannot be accelerated indefinitely but oscillates in real space) and the formation of gap solitons [4] (localized wave packets arising from the balance between negative-mass dispersion and repulsive interaction). Both of these phenomena have recently been observed in a Bose-Einstein condensate (BEC) in an optical lattice [5,6].

In this Letter, we show that yet another system, a BEC confined in a rotating harmonic-plus-quartic potential, exhibits a Bloch band structure, and we investigate the associated novel phenomena. Seemingly this system has no periodic structure but may be considered to be a quasi-1D periodic system in the following sense. When the rotating frequency of the potential is high, the quartic potential, $\propto r^4$, together with the centrifugal potential, $\propto -r^2$, produces a Mexican-hat-shaped potential [7] whose minima form a quasi-1D toroidal geometry. Under such circumstances any perturbation $V(\theta)$ that is needed to drive the system into rotation by breaking the axisymmetry serves as a "periodic" potential since $V(\theta) = V(\theta + 2\pi)$, where θ denotes the azimuthal angle.

In the present system, we show that by controlling the frequency of the rotating drive or the strength of the interaction, we can manipulate the condition of Bragg"s law, thereby nucleating or removing vortices adiabatically. In contrast to a method that invokes dynamical instabilities [8,9], we can create the vortex state without heating the atomic cloud. Schemes that adiabatically nucleate vortices have also been proposed in Refs. [10–14]. We also show that a localized state is generated even with repulsive interactions, in a manner analogous to gap soliton formation in periodic systems [4].

We begin by discussing a BEC in a 1D ring to illustrate the essence of the phenomena. We assume that a rotating potential takes the form $V(\theta, t) = \varepsilon \cos n(\theta - \Omega t)$, where n is an integer. In a frame rotating at frequency Ω, the potential V becomes time independent, and the Gross-Pitaevskii (GP) equation is given by

$$\left(-\frac{\partial^2}{\partial\theta^2} + i\Omega\frac{\partial}{\partial\theta} + \varepsilon\cos n\theta + \gamma|\psi_{1D}|^2\right)\psi_{1D} = \mu\psi_{1D}, \quad (1)$$

where energy and time are measured in units of $\hbar^2/(2mR^2)$ and $2mR^2/\hbar$ with m and R being the atomic mass and the radius of the ring, and γ characterizes the strength of the interaction. The wave function is normalized as $\int_0^{2\pi} |\psi_{1D}|^2 d\theta = 1$.

First, let us consider the noninteracting case ($\gamma = 0$). By the gauge transformation $\phi \equiv e^{-i\Omega\theta/2}\psi_{1D}$, Eq. (1) takes the form of the Mathieu equation $(-\partial_\theta^2 + \varepsilon\cos n\theta)\phi = E\phi$, where $E \equiv \mu + \Omega^2/4$ plays the role of the total energy in our Bloch band picture. From the Bloch theorem and the single valuedness of ψ_{1D}, the solution is found to satisfy $\phi(\theta + \Theta_0) = e^{i(p-\Omega/2)\Theta_0}\phi(\theta)$, with $\Theta_0 \equiv 2\pi/n$ being the period of the potential V and the integer p is the winding number $\int_0^{2\pi} \partial_\theta \arg\psi_{1D} d\theta/2\pi$ [15]. It follows that $p - \Omega/2$ may be regarded as the quasimomentum, indicating that we can move in the quasimomentum space by changing Ω. Figure 1 shows E and the angular momentum $\langle L\rangle = -i\int_0^{2\pi} \psi_{1D}^* \partial_\theta \psi_{1D} d\theta$ as functions of Ω for the first and second Bloch bands. The Bloch band structure in Fig. 1 indicates that if we adiabatically increase or *decrease* Ω across $\Omega = 2$, the nonvortex state $\psi_{1D} \simeq 1/\sqrt{2\pi}$ transforms to the doubly quantized vortex state $\psi_{1D} \simeq e^{2i\theta}/\sqrt{2\pi}$ and vice versa. The time scale of the adiabatic change must be much longer than the inverse energy gap $\simeq \varepsilon^{-1}$.

When $|\gamma| \gtrsim \varepsilon$, the system exhibits hysteretic behavior and a loop structure emerges in the Bloch bands [16]. We see in Fig. 1 that the first and second bands form loops for $\gamma = 1$ and -1, respectively; hence the adiabatic nucleation of vortices is not possible with, respectively, increasing and decreasing Ω because the nonlinear Landau-Zener transition [16,17] occurs no matter how slow the

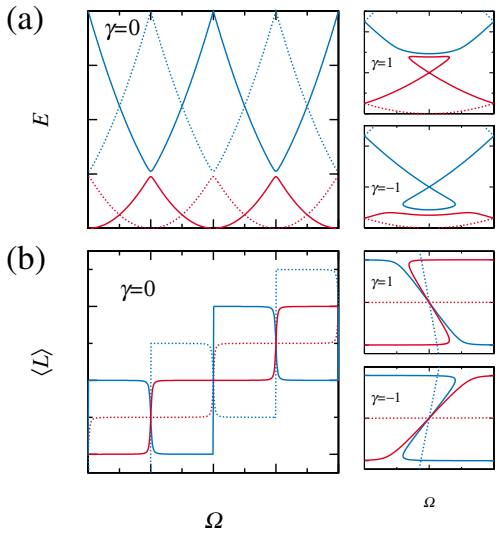

FIG. 1 (color). (a) $E \equiv \mu + \Omega^2/4$ and (b) $\langle L\rangle \equiv -i\int \psi_{1D}^* \times \partial_\theta \psi_{1D} d\theta$ of the first (red curves) and the second (blue curves) Bloch bands for the noninteracting (main panels) and interacting (right panels) BECs in a 1D ring described by Eq. (1) with $V(\theta) = 0.1\cos 2\theta$. Since $V(\theta)$ has the twofold symmetry, there are two independent branches with even and odd values of $\langle L\rangle$ [15], which are shown by the solid and dotted curves.

change of Ω. It can be shown that the states on the loop have dynamical instability [18] that breaks the symmetry of the system $|\psi_{1D}(\theta)| = |\psi_{1D}(\theta + \Theta_0)|$. This instability is similar to the one that forms gap solitons in a BEC in an optical lattice [19].

We now consider a BEC in a harmonic-plus-quartic potential with a rotating stirrer. We assume a tight pancake-shaped trap such that the axial trapping energy $\hbar\omega_z$ is much larger than other characteristic energies and that the system is effectively 2D. The external potential in the corotating frame of reference takes the form $V(\mathbf{r}) = r^2/2 + Kr^4/4 + \varepsilon r^2 \cos 2\theta$, where K is a constant and the third term $\varepsilon(x^2 - y^2)$ is a stirring potential, which can be produced by laser beams propagating in the z direction. Such an anharmonic potential was theoretically considered in Refs. [7,20,21] and has recently been realized experimentally [22]. We normalize the length, time, energy, and wave function by $d_0 \equiv (\hbar/m\omega_\perp)$, $\omega_\perp^{-1}$, $\hbar\omega_\perp$, and $\sqrt{N}/d_0$, respectively, with $\omega_\perp$ and N being the frequency of the radial harmonic trap and the number of atoms. The wave function is then normalized as $\int |\psi_{2D}|^2 d\mathbf{r} = 1$. The time-dependent GP equation in the frame corotating with the stirring potential at frequency Ω is given by

$$i\frac{\partial \psi_{2D}}{\partial t} = \left[-\frac{1}{2}\nabla^2 + i\Omega\frac{\partial}{\partial\theta} + V(\mathbf{r}) + g|\psi_{2D}|^2\right]\psi_{2D}, \quad (2)$$

where $g = [\omega_z/(2\pi\omega_\perp)]^{1/2} 4\pi N a/d_0$ characterizes an effective strength of interaction in 2D [23] with a being the s-wave scattering length.

When $\Omega \gg 1$, the system described by Eq. (2) can be approximated by a quasi-1D ring [7]. Assuming $\psi_{2D} \simeq f(r)e^{i\ell\theta}/\sqrt{2\pi}$, we find that an effective potential for the radial wave function is given by $\ell^2/(2r^2) + r^2/2 + Kr^4/4$. This potential has a minimum at $r \simeq (\ell^2/K)^{1/6}$ for $\ell \gg 1$ and the effective frequency around it is $\omega_{\rm eff} \simeq \sqrt{6}(\ell K)^{1/3}$. If $\omega_{\rm eff}$ is much larger than other characteristic frequencies, the dynamics of $f(r)$ can be ignored. After normalization of the time by $\rho^{-2} \equiv \int r|f|^2 r^{-2} dr$, the equation of motion for θ reduces to Eq. (1), where γ is given by $2g\rho^2 \int r|f|^4 dr$. Thus, the system described by Eq. (2) exhibits the quasi-1D circular flow for large angular momentum [7], and we expect that a Bloch band structure emerges. We show below that this is true even for $\Omega \sim 1$ and $\ell \sim 1$.

Figure 2(a) shows the angular momentum $\langle L\rangle = -i \times \int \psi_{2D}^* \partial_\theta \psi_{2D} d\mathbf{r}$ and the density and phase profiles (insets) of the noninteracting stationary states of Eq. (2) [24]. We find that the behavior of $\langle L\rangle$ is similar to that in Fig. 1(b). When we start from the ground state with $\langle L\rangle = 0$ (1-1), two vortices enter at $\Omega \simeq 1.57$ (1-2), producing a doubly quantized vortex (1-3) [20]. Increasing the rotation fre-

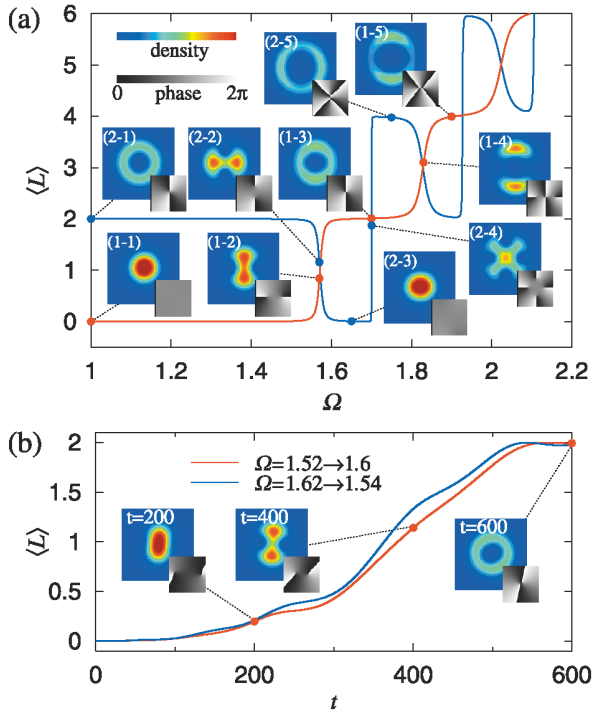

FIG. 2 (color). (a) Angular momentum $\langle L\rangle$ versus rotation frequency Ω of the stationary states of Eq. (2) with $g = 0$, $K = 1$, and $\varepsilon = 0.02$. The images (1-1)–(1-5) and (2-1)–(2-5) correspond to the branches indicated by the red and blue curves. (b) Time evolutions with $g = 0$, $K = 1$, and an additional dissipation parameter $\lambda = 0.03$, where Ω is changed linearly from 1.52 to 1.6 (red curve) and from 1.62 to 1.54 (blue curve) during $0 \le t \le 600$. The initial state is the nonvortex ground state. The parameter ε is linearly ramped up from 0 to 0.04 during $0 \le t \le 200$, kept at 0.04 during $200 \le t \le 400$, and ramped down from 0.04 to 0 during $400 \le t \le 600$ to suppress nonadiabatic disturbances. The size of the images is 5×5 in units of $(\hbar/m\omega_\perp)^{1/2}$.

quency Ω further, we can nucleate two more vortices in the condensate [(1-4) and (1-5)]. If we follow the branch starting from $\langle L\rangle = 2$ (2-1), the two vortices escape out of the condensate with *increasing* Ω [(2-2) and (2-3)] and then four vortices enter at $\Omega \simeq 1.7$ (2-4). As in the 1D case [15], the changes of the vorticity are even numbers because of the twofold symmetry of $V(\mathbf{r})$. It should be noted that the Bloch band picture holds even for the nonrotating gas, while the ring-shaped profile manifests itself only if the gas is rotating [cf. (1-1) and (2-3)].

The frequencies at which the Bragg reflection occurs in Fig. 2(a) are different from those in Fig. 1. The difference arises from the dispersion relation of the vortex states in 2D, i.e., the relation between the energy and angular momentum. In the 1D case, the energy is given by $E_m^{\rm 1D} = \int d\theta[\psi_m^{\rm 1D*}(-\partial_\theta^2 + i\Omega\partial_\theta)\psi_m^{\rm 1D} + \gamma|\psi_m^{\rm 1D}|^4/2] = m^2 - \Omega m + \gamma/(4\pi)$ for $\psi_m^{\rm 1D} = e^{im\theta}/\sqrt{2\pi}$. The Bragg reflection between $\psi_m^{\rm 1D}$ and $\psi_{m+2}^{\rm 1D}$ occurs when $E_m^{\rm 1D} = E_{m+2}^{\rm 1D}$, i.e., $\Omega = 2m + 2$. In the 2D case, we employ a variational wave function $\psi_m^{\rm 2D} = (\pi|m|!)^{-1/2} d_m^{-|m|-1} r^{|m|} \exp[-r^2/(2d_m^2) + im\theta]$ to obtain $E_m^{\rm 2D} = (|m| + 1)(d_m^{-2} + d_m^2)/2 + K(|m| + 1)(|m| + 2)d_m^4/4 - \Omega m + g(2|m|)!/[2^{2|m|+2} \times \pi|m|!^2 d_m^2]$, where the variational parameter d_m is determined from $\partial E_m^{\rm 2D}/\partial d_m = 0$. When $K = 1$ and $g = 0$, the condition for Bragg reflection to occur between $\psi_m^{\rm 2D}$ and $\psi_{m+2}^{\rm 2D}$ ($E_m^{\rm 2D} = E_{m+2}^{\rm 2D}$) for $m = 0$, 2, and 4 is satisfied at $\Omega = 1.58$, 1.83, and 2.03, respectively, which are in good agreement with the numerical results in Fig. 2(a) (corresponding to the points at which the red and blue curves cross, with $\langle L\rangle$ changing by ± 2).

The energy gap can also be obtained by a variational method. The matrix element of the stirring potential, for example, between $\psi_0^{\rm 2D}$ and $\psi_2^{\rm 2D}$ is calculated to be $|\int d\mathbf{r}\psi_2^{\rm 2D*}\psi_0^{\rm 2D}\varepsilon r^2\cos 2\theta| \simeq 0.46\varepsilon$ for $K = 1$. The energy gap at $\Omega \simeq 1.57$ is then given by $\simeq 0.92\varepsilon$, which also agrees very well with the numerical result $\simeq 0.91\varepsilon$.

The Bloch band structure in Fig. 2(a) indicates that if we prepare the nonvortex state at $\Omega \lesssim 1.55$ and adiabatically increase Ω to above $\Omega \simeq 1.6$, we obtain a doubly quantized vortex state by following the red curve. Interestingly, we can nucleate vortices also by *decreasing* Ω, that is, by preparing a nonvortex state for $1.6 \lesssim \Omega \lesssim 1.7$ and decreasing Ω to below $\Omega \simeq 1.55$ by following the second Bloch band (blue curve). Figure 2(b) illustrates these adiabatic processes; here to take into account the effect of dissipation on the adiabatic processes, we replace i with $i - \lambda$ on the left-hand side of Eq. (2), where a constant λ is taken to be 0.03 [25]. We prepare the nonvortex ground state with $g = 0$ and gradually ramp up Ω from 1.52 to 1.6 [red curve in Fig. 2(b)], or ramp it down from 1.62 to 1.54 (blue curve). As expected, two density holes with phase singularities come from infinity and unite to form a doubly quantized vortex. We note that the behaviors in Fig. 2(b) are almost the same as for the dissipation-free case ($\lambda = 0$, data not shown), indicating that the process is robust against dissipation. The energy gap between the first and second Bloch bands at $\Omega \simeq 1.57$ is $\simeq 0.036$ for $\varepsilon = 0.04$. According to the Landau-Zener formula, the transition probability between the energy gap is below 1% in the situation in Fig. 2(b), in agreement with our numerical result.

In the case of $g \neq 0$, the interaction bends the Bloch bands as shown in Fig. 3(a), yielding hysteresis as in the 1D case. We note that the region of Ω in which the Bragg reflection occurs is shifted due to the interaction. The shift is attributed to the difference in interaction energies between the nonvortex and vortex states. To show this we again employ the variational wave function $\psi_m^{\rm 2D}$. We find that the condition for the Bragg reflection to occur between $\psi_0^{\rm 2D}$ and $\psi_2^{\rm 2D}$, i.e., $E_0^{\rm 2D} = E_2^{\rm 2D}$, is satisfied at $\Omega = 1.53$ for $g = 1.6$ and $\Omega = 1.64$ for $g = -1.6$, in qualitative agreement with the shifts shown in Fig. 3(a). Since the interaction term of $E_m^{\rm 1D}$ is independent of m, the shift does not occur in 1D (see Fig. 1).

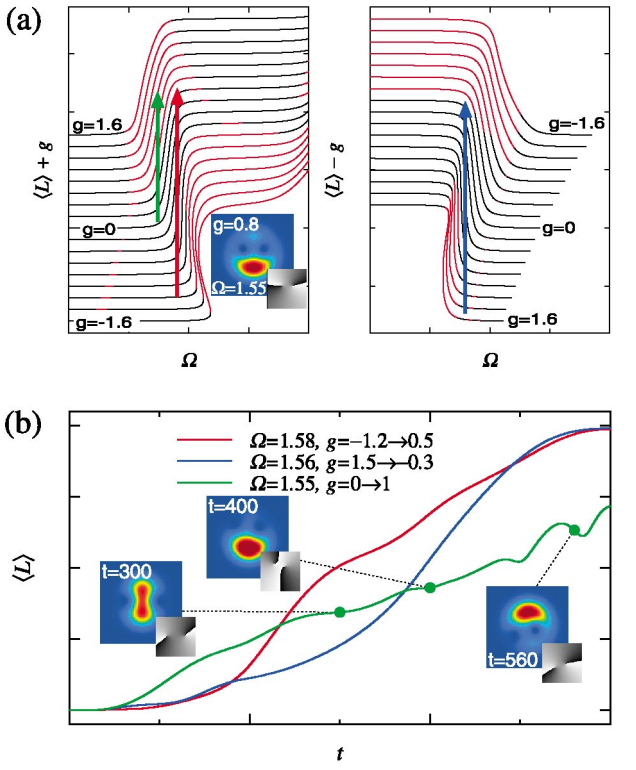

FIG. 3 (color). (a) The g dependence of the first and second bands (left and right panels) with $K = 1$ and $\varepsilon = 0.02$, where the ordinates are offset by $\pm g$ for clarity. The dynamically unstable regions are indicated by the red curves. The inset shows a localized stationary state—a gap soliton—formed near the first band at $g = 0.8$ and $\Omega = 1.55$. (b) Time evolutions with $\lambda = 0.03$ and $K = 1$, where g is linearly ramped from -1.2 to 0.5 with $\Omega = 1.58$ [red curve, corresponding to the red arrow in (a)], from 1.5 to -0.3 with $\Omega = 1.56$ (blue curve, blue arrow), and from 0 to 1 with $\Omega = 1.55$ (green curve, green arrow). The change in ε for the red and blue curves is the same as that in Fig. 2(b). For the green curve, $\varepsilon = 0.04$ is maintained during $200 \leq t \leq 600$ and a small perturbation to break the axisymmetry is added to the initial state.

The shift in the position of the Bragg reflection implies the possibility of the adiabatic nucleation of vortices at *fixed* Ω by changing the strength of the interaction using, e.g., the Feshbach resonance [26]. For example, at $\Omega \simeq 1.58$, the first Bloch band has angular momentum $\langle L \rangle \simeq 0$ for $g \lesssim -1$ [left panel in Fig. 3(a)], which continuously increases to $\langle L \rangle \simeq 2$ with an increase in the interaction from attractive to repulsive (red arrow). Similarly, there is a region in which $\langle L \rangle$ changes from 0 to 2 as g decreases from positive to negative [blue arrow in the right panel in Fig. 3(a)]. No dynamical instability is present for the red and blue arrows. Figure 3(b) illustrates these results, where the initial state is the nonvortex ground state and the strength of the interaction is gradually changed with Ω held fixed (red and blue curves). We find that the two vortices are nucleated in a manner similar to that in Fig. 2(b). The repulsive-to-attractive case is particularly interesting because the attractive interaction is usually considered to hinder vortex nucleation [21].

The adiabatic theorem breaks down when the path enters the region of dynamical instability. A notable example is shown by the green arrow in Fig. 3(a), where dynamical instability arises for $g \gtrsim 0.6$ at $\Omega \simeq 1.55$. This instability causes a twofold symmetric state [like the inset (1-2) of Fig. 2(a)] to transform into a localized state shown in the inset of Fig. 3(a); the localized state undergoes a center-of-mass motion in order to preserve the angular momentum [27]. This localization is due to the interplay between repulsive interaction and negative-mass dispersion around the edge of the Brillouin zone. The localized state can therefore be regarded as an analog of the gap soliton in a periodic system [4]. The green curve in Fig. 3(b) demonstrates the time evolution corresponding to the path shown by the green arrow in Fig. 3(a). The twofold symmetry shown in the inset at $t = 300$ is broken in the course of vortex nucleation, giving rise to two localized states, shown in the insets at $t = 400$ and $t = 560$.

In conclusion, we have shown that the Bloch band structure arises in a BEC confined in a harmonic-plus-quartic potential with a rotating drive, which enables us to nucleate vortices adiabatically. The physical mechanism of vortex nucleation is very similar to Bragg reflection at the edge of the Brillouin zone. Interestingly, we can nucleate vortices not only by increasing the stirring frequency but also by decreasing it, or by changing the strength of the interaction at a fixed stirring frequency, which may be called a "Feshbach-induced Bragg reflection." The adiabatic processes are shown to be robust against dissipation due, e.g., to thermal processes. Spontaneous localization of the rotating cloud is predicted, which indicates the emergence of a gap soliton.

This work was supported by the Special Coordination Funds for Promoting Science and Technology, a 21st Century COE program at Tokyo Tech "Nanometer-Scale Quantum Physics," and a Grant-in-Aid for Scientific Research (Grant No. 15340129) from the Ministry of Education, Science, Sports, and Culture of Japan.

[1] J. M. Ziman, *Principles of the Theory of Solids* (Cambridge University Press, New York, 1972).
[2] For review, see P. S. Jessen and I. H. Deutsch, Adv. At. Mol. Opt. Phys. **37**, 95 (1996).
[3] K. K. Likharev and A. B. Zorin, J. Low Temp. Phys. **59**, 347 (1985).
[4] P. Meystre, *Atom Optics* (Springer-Verlag, New York, 2001), and references therein.
[5] O. Morsch *et al.*, Phys. Rev. Lett. **87**, 140402 (2001).
[6] B. Eiermann *et al.*, Phys. Rev. Lett. **92**, 230401 (2004).
[7] K. Kasamatsu *et al.*, Phys. Rev. A **66**, 053606 (2002).
[8] S. Sinha and Y. Castin, Phys. Rev. Lett. **87**, 190402 (2001).
[9] K. W. Madison *et al.*, Phys. Rev. Lett. **86**, 4443 (2001).
[10] R. Dum *et al.*, Phys. Rev. Lett. **80**, 2972 (1998).
[11] B. M. Caradoc-Davies *et al.*, Phys. Rev. Lett. **83**, 895 (1999).
[12] J. E. Williams and M. J. Holland, Nature (London) **401**, 568 (1999); M. R. Matthews *et al.*, Phys. Rev. Lett. **83**, 2498 (1999).
[13] M. Nakahara *et al.*, Physica (Amsterdam) **284B–288B**, 17 (2000); A. E. Leanhardt *et al.*, Phys. Rev. Lett. **89**, 190403 (2002).
[14] B. Damski *et al.*, J. Phys. B **35**, 4051 (2002).
[15] Since the unit "reciprocal lattice vector" is $2\pi/\Theta_0 = n$, Bragg reflection occurs only between states whose angular momenta differ by $n, 2n, \ldots$ (Bragg's law). Consequently there are n independent branches corresponding to $p = 0, \ldots, n-1$ modulo n. We note that the wave function of each branch differs only by a θ-dependent factor $e^{ip\theta}$.
[16] B. Wu and Q. Niu, Phys. Rev. A **61**, 023402 (2000).
[17] The adiabatic theorem is generalized to nonlinear systems in J. Liu *et al.*, Phys. Rev. Lett. **90**, 170404 (2003).
[18] A BEC in an optical lattice exhibits dynamical instability even when there is no loop in the Bloch bands, as shown in B. Wu and Q. Niu, Phys. Rev. A **64**, 061603(R) (2001).
[19] V. V. Konotop and M. Salerno, Phys. Rev. A **65**, 021602(R) (2002).
[20] E. Lundh, Phys. Rev. A **65**, 043604 (2002).
[21] The fact that a vortex can exist in a BEC with weak attractive interactions is also pointed out in E. Lundh *et al.*, Phys. Rev. Lett. **92**, 070401 (2004).
[22] V. Bretin *et al.*, Phys. Rev. Lett. **92**, 050403 (2004).
[23] Y. Castin and R. Dum, Eur. Phys. J. D **7**, 399 (1999).
[24] Here vortices are defined as localized density depletions that have phase singularities. The core size of a vortex is kept from diverging in the limit of $g = 0$ due to the presence of a trapping potential.
[25] S. Choi *et al.*, Phys. Rev. A **57**, 4057 (1998).
[26] S. Inouye *et al.*, Nature (London) **392**, 151 (1998).
[27] Dynamical instability due to the presence of symmetry-broken low-lying states is also discussed in H. Saito and M. Ueda, Phys. Rev. Lett. **89**, 190402 (2002); Phys. Rev. A **69**, 013604 (2004).